Supplemental Figure 1: Whole-brain pattern of working memory-related activity.

Main effects for the contrast of E_RCJ>EC_RJ (see Figure 1 for details) across frontal, parietal, and temporal cortices (red) at $p<0.05$, FWE-corrected for multiple comparisons. Our dlPFC region of interest is highlighted in yellow.

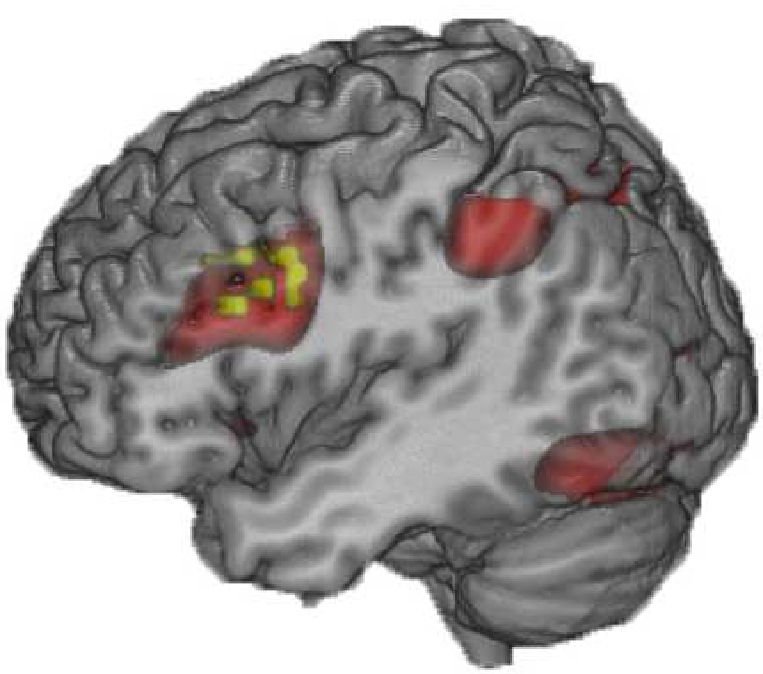

Supplemental Figure 2: Habitual use of reappraisal is associated with decreased symptoms of anxiety and depression in the context of stress. *At intermediate and high levels of stress, increased use of habitual reappraisal is associated with fewer mood and anxiety symptoms ($p<0.001$).*

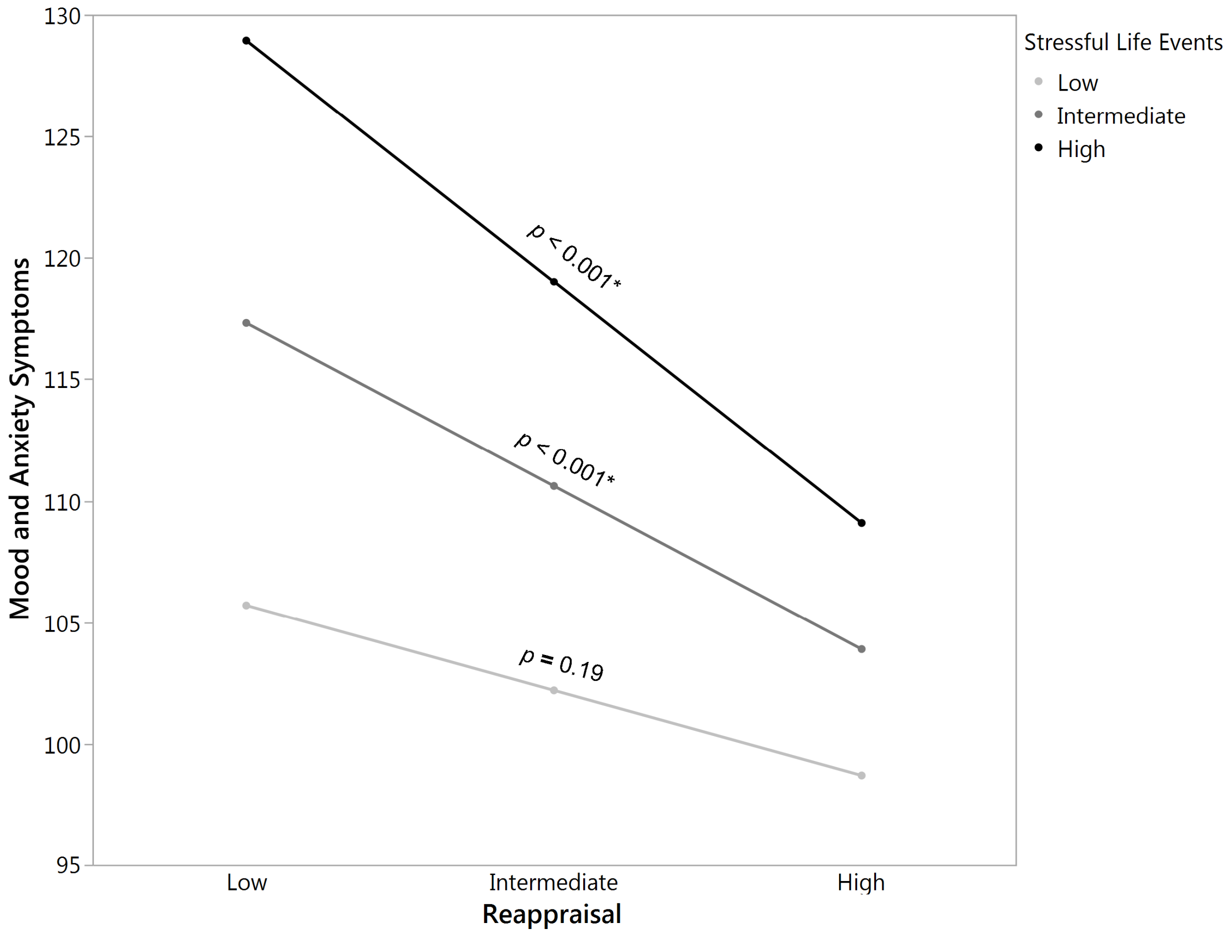

Supplemental Table 1

	N (%)
One Diagnosis	24 (12.9)
More Than One Diagnosis	19 (10.2)
Major Depressive Disorder	21 (11.3)
Bipolar Disorder	4 (2.2)
Panic Disorder	11 (5.9)
Agoraphobia	8 (4.3)
Generalized Anxiety Disorder	4 (2.2)
Social Anxiety Disorder	2(1.1)
Obsessive Compulsive Disorder	3 (1.6)
Alcohol Abuse or Dependence	13 (7.0)
Other Substance Abuse or Dependence	7 (3.8)
Eating Disorder	2 (1.1)
Missing	1 (0.5)

Supplemental Methods

Working Memory fMRI Paradigm

Activity of the dlPFC was measured during BOLD fMRI using an event-related working memory paradigm adapted from Tan et al. (Tan et al., 2007). The paradigm included 10 trials for each of 6 different conditions, including 3 control conditions, consisting only of a 3s response phase, and 3 working memory (WM) conditions, consisting of a 0.5s encoding phase followed by a 4s maintenance interval and a 3s response phase (Fig. 1). Control and WM conditions were interleaved with jittered rest intervals lasting 4s to 8.5s for a total scan length of 11m 48s. Responses were recorded via an MR-compatible button box using the index (left button) and middle (right button) fingers of the dominant hand.

During the control conditions, participants performed 1) a simple motor task (M) in which they pressed either the left or the right button according to a prompt, 2) a numerical size judgment task (J) in which they chose the number on the left or right based on an instruction to choose either the larger or the smaller number, and 3) a numerical computation and size judgment task (CJ) in which they performed a numerical subtraction of 2 or 3 from either the left or right number, and made a numerical size judgment as instructed.

In the first WM condition, participants viewed 2 numbers during the brief encoding phase, then recalled the numbers and performed a numerical size judgment as instructed (E_RJ). In the second WM condition, the participants additionally performed subtraction of 2 or 3 from one of the remembered numbers as indicated before making the numerical size judgment during recall (E_RCJ). In the final WM condition, participants performed subtraction of 2 or 3 from one of the 2 numbers during the brief encoding phase, then recalled the resulting two numbers and performed a numerical size judgment as instructed during the response phase after the maintenance interval (EC_RJ). In each WM condition trial, all the numbers were single digits from 0 to 9; the two numbers on which the numerical size judgment was ultimately performed (after numerical computation if applicable) were equally balanced across 0 to 9, and equally likely to differ by either 1 or 3 units. Numerical computation was equally likely on the left or right number, with correct responses equally balanced on the left or right, and equally likely to be the larger or smaller number for each WM trial type. The trials were performed in an order that was optimized using a sequencing program (Wager & Nichols, 2003).

BOLD fMRI data acquisition

Each participant was scanned using one of two identical research-dedicated GE MR750 3T scanner equipped with an eight-channel head coil for parallel imaging at high bandwidth. A semiautomated high-order shimming program was used to ensure global field homogeneity. A series of 34 interleaved axial functional slices aligned with the anterior commissure–posterior commissure plane were acquired for full-brain coverage using an inverse-spiral pulse sequence to reduce susceptibility artifact. To allow for spatial registration of each participant's data to a standard coordinate system, structural images were acquired in 34 axial slices co-planar with the functional scans. For additional details on data acquisition parameters please see (Ahs, Davis, Gorka, & Hariri, 2014).

BOLD fMRI data preprocessing

Preprocessing was conducted using SPM8 (www.fil.ion.ucl.ac.uk/spm). Images for each participant were slice-time corrected, realigned to the first volume in the time series to correct for head motion, spatially normalized into a standard stereotactic space (Montreal Neurological Institute template) using a 12-parameter affine model (final resolution of functional images = 2mm isotropic voxels) and smoothed to minimize noise and residual differences in gyral anatomy with a Gaussian filter set at 6mm full-width at half-maximum. Next, the Artifact Detection Tool was used to generate regressors accounting for the possible confounding effects of volumes with large motion deflections (http://www.nitrc.org/projects/artifact_detect). Specifically, individual whole-brain BOLD fMRI volumes varying significantly from mean-volume signal intensity variation (i.e., within volume mean signal of greater or less than 4 standard deviations of mean signal of all volumes in time series) or individual volumes where scan-to-scan movement exceeded 2mm translation or 2º rotation in any direction were assigned a lower weight in analyses. Of the 216 participants with available fMRI data, 13 participants had >5% outlier volumes and were excluded from further analyses. Data for another 14 participants were excluded from further analyses for poor task performance reflected as less than 75% overall accuracy or below 50% accuracy on any trial type. Data for an additional 3 participants were lost due to scanner malfunction. Thus, our primary analyses were conducted in 186 participants.

References

Ahs, F., Davis, C. F., Gorka, A. X., & Hariri, A. R. (2014). Feature-based representations of emotional facial expressions in the human amygdala. *Social Cognitive and Affective Neuroscience*, *9*(9), 1372–1378. doi:10.1093/scan/nst112

Tan, H.-Y., Chen, Q., Goldberg, T. E., Mattay, V. S., Meyer-Lindenberg, A., Weinberger, D. R., & Callicott, J. H. (2007). Catechol-O-methyltransferase Val158Met modulation of prefrontal-parietal-striatal brain systems during arithmetic and temporal transformations in working memory. *The Journal of Neuroscience : The Official Journal of the Society for Neuroscience*, *27*(49), 13393–401. doi:10.1523/JNEUROSCI.4041-07.2007

Wager, T. D., & Nichols, T. E. (2003). Optimization of experimental design in fMRI: A general framework using a genetic algorithm. *NeuroImage*, *18*(2), 293–309. doi:10.1016/S1053-8119(02)00046-0